tration of serotonin S_2 receptors in monkeys whose behavior is socially adapted as well as a low concentration in aggressive, socially uncooperative animals (*15*). In contrast, structures in the dorsolateral region are involved in other domains of cognition concerning extrapersonal space, objects, language, and arithmetic (*16*). These structures are largely intact in Gage-like patients, thus accounting for the patients' normal performance in traditional neuropsychologic tests that are aimed at such domains.

The assignment of frontal regions to different cognitive domains is compatible with the idea that frontal neurons in any of those regions may be involved with attention, working memory, and the categorization of contingent relationships regardless of the domain (*17*). This assignment also agrees with the idea that in non–brain-damaged individuals the separate frontal regions are interconnected and act cooperatively to support reasoning and decision making. The mysteries of frontal lobe function are slowly being solved, and it is only fair to establish, on a more substantial footing, the roles that Gage and Harlow played in the solution.

REFERENCES AND NOTES

1. J. M. Harlow, *Pub. Mass. Med. Soc.* **2**, 327 (1868).
2. P. Broca, *Bull. Soc. Anthropol.* **6**, 337 (1865); C. Wernicke, *Der aphasische Symptomencomplex* (Cohn und Weigert, Breslau, Poland, 1874). A remarkable number of basic insights on the functional specialization of the human brain, from motor function to sensory perception and to spoken and written language, came from the description of such cases mostly during the second half of the 19th century. The cases usually acted as a springboard for further research, but on occasion their significance was overlooked, as in the case of Gage. Another such example is the description of color perception impairment (achromatopsia) caused by a ventral occipital lesion, by D. Verrey [*Arch. Ophthalmol.* (*Paris*) **8**, 289 (1888)]. His astonishing finding was first denied and then ignored until the 1970s.
3. Reasoning and social behavior were deemed inextricable from ethics and religion and not amenable to biological explanation.
4. The reaction against claims for brain specialization was in fact a reaction against phrenological doctrines, the curious and often unacknowledged inspiration for many of the early case reports. The views of E. Dupuy exemplify the attitude [*Examen de Quelques Points de la Physiologie du Cerveau* (Delahaye, Paris, 1873); M. MacMillan, *Brain Cognit.* **5**, 67 (1986)].
5. D. Ferrier, *Br. Med. J.* **1**, 399 (1878).
6. The first measurements were those necessary to construct Gage's Talairach stereotactic space and deform a three-dimensional, computerized tomography skull: the maximum length of the skull, the maximum height of the skull above the inion-glabella line, the distance from this line to the floor of the middle fossa, the maximum width of the skull, and the position of the section contour of Gage's skull relative to the inion-glabella line. The second measurements were those necessary to construct the entry and exit areas: on the top external view, the measure of edges of the triangular exit hole; on the internal view the distances from its three corners to the mid-sagittal line and to the nasion; the distance from the borders of the hole to the fracture lines seen anteriorly and posteriorly to this hole; and the dimensions of the entry hole at the level of the orbit.
7. Thin-cut standard computerized tomography image of a cadaver head obtained at North Carolina Memorial Hospital.
8. We introduced the following changes to the method described by P. Fox, J. Perlmutter, and M. Raichle [*J. Comput. Assist. Tomogr.* **9**, 141 (1985)]. We calculated the mean distance from the anterior commissure (AC) to the posterior commissure (PC) in a group of 27 normal brains and used that distance for Gage (26.0 mm). We also did not consider the AC-frontal pole and the PC-occipital pole distances as equal because our group of normals had a mean difference of 5 mm between the two measures, and Talairach himself did not give these two measurements as equal [J. Talairach and G. Szikla, *Atlas d'Anatomie Stereotaxique du Telencephale* (Masson, Paris, 1967); J. Talairach and P. Tournoux, *Co-Planar Stereotaxic Atlas of the Human Brain* (Thieme, New York, 1988)]. We introduced an anterior shift of 3% to the center of the AC-PC line and used that point as the center of the AC-PC segment. This shift meant that the anterior sector of Talairach's space was 47% of the total length and that the posterior was 53%. We had no means of calculating the difference between the right and left width of Gage's brain; therefore, we assumed them to be equal.
9. H. Damasio and R. Frank, *Arch. Neurol.* **49**, 137 (1992).
10. There were two reasons to allow the vector this close to the mandible: (i) The zygomatic arch and the coronoid process were never more than 2 cm apart; (ii) we assumed that, in reality, this distance might have been larger if the mouth were open or if the mandible, a movable structure, had been pushed by the impact of the iron rod.
11. The final dimensions of Phineas Gage's Talairach space were as follows: total length, 171.6 mm; total height, 111.1 mm; and total width, 126.5 mm. Comparing these dimensions to a group of 27 normal subjects, we found that in seven cases at least two of the dimensions were close to those of Phineas Gage [mean length, 169.9 mm (SD, 4.1); mean height, 113.6 (SD, 2.3), mean width, 125 (SD, 3.9). The seven brains were fitted with the possible trajectories to determine which brain areas were involved. There were no significant differences in the areas of damage. The modeling we present here was performed on subject 1600LL (length, 169 mm; height, 115.2 mm; width, 125.6 mm).
12. Data from the Lesion Registry of the University of Iowa's Division of Cognitive Neuroscience as of 1993.
13. P. Eslinger and A. R. Damasio, *Neurology* **35**, 1731 (1985); J. L. Saver and A. R. Damasio, *Neuropsychologia* **29**, 1241 (1991); A. R. Damasio, D. Tranel, H. Damasio, in *Frontal Lobe Function and Dysfunction*, H. S. Levin, H. M. Eisenberg, A. L. Benton, Eds. (Oxford Univ. Press, New York, 1991), pp. 217–229; S. Dehaene and J. P. Changeux, *Cereb. Cortex* **1**, 62 (1991).
14. P. S. Goldman-Rakic, in *Handbook of Physiology; The Nervous System*, F. Plum, Ed. (American Physiological Society, Bethesda, MD, 1987), vol. 5, pp. 373–401; D. N. Pandya and E. H. Yeterian, in *The Prefrontal Cortex: Its Structure, Function and Pathology*, H. B. M. Uylings, Ed. (Elsevier, Amsterdam, 1990); H. Barbas and D. N. Pandya, *J. Comp. Neurol.* **286**, 253 (1989).
15. M. J. Raleigh and G. L. Brammer, *Soc. Neurosci. Abstr.* **19**, 592 (1993).
16. M. Petrides and B. Milner, *Neuropsychologia* **20**, 249 (1982); J. M. Fuster, *The Prefrontal Cortex* (Raven, New York, ed. 2, 1989); M. I. Posner and S. E. Petersen, *Annu. Rev. Neurosci.* **13**, 25 (1990).
17. P. S. Goldman-Rakic, *Sci. Am.* **267**, 110 (September 1992); A. Bechara, A. R. Damasio, H. Damasio, S. Anderson, *Cognition* **50**, 7 (1994); A. R. Damasio, *Descartes' Error: Emotion, Reason and the Human Brain* (Putnam, New York, in press).
18. We thank A. Paul of the Warren Anatomical Museum for giving us access to Gage's skull. Supported by National Institute of Neurological Diseases and Stroke grant PO1 NS19632 and by the Mathers Foundation.

RESEARCH ARTICLE

Highly Conjugated, Acetylenyl Bridged Porphyrins: New Models for Light-Harvesting Antenna Systems

Victor S.-Y. Lin, Stephen G. DiMagno, Michael J. Therien*

A new class of porphyrin-based chromophore systems has been prepared from ethyne-elaborated porphyrin synthons through the use of metal-mediated cross-coupling methodologies. These systems feature porphyrin chromophores wired together through single ethynyl linkages. This type of topological connectivity affords exceptional electronic interactions between the chromophores which are manifest in their room temperature photophysics, optical spectroscopy, and electrochemistry; these spectroscopic signatures indicate that these species model many of the essential characteristics of biological light-harvesting antenna systems.

The optical, electronic, and photophysical properties of porphyrins have made these molecules desirable targets for incorporation into supramolecular systems and polymers due to their central importance in the developing biomimetic chemistry of multichromophoric assemblies in biology as well as for potential application in sensing (*1*), opto-electronic (*2*), magnetic (*3*), artificial photosynthetic (*4*, *5*), catalytic (*6*), and photosensitizing-pharmaceutical materials (*7*). A common objective in the fabrication of many of these macromolecular systems has been the facile organization of the individual porphyrin molecules comprising the multichromophoric assembly such that they exhibit maximal mutual electronic and excitonic interactions.

Nature is replete with systems where large ground- and excited-state electronic interactions between chromophores are essential for biological function. The photosynthetic antenna systems, which play crucial roles in both light harvesting and energy transfer, serve as archetypal examples illustrating the application of highly coupled chromophores in biology. Effective biomimetic modeling of the natural photon-gathering machinery is dependent upon overcoming several obstacles, two of which include: (i) fabricating systems that have high molar absorptivity throughout the visible and high-energy near-infrared regions of the electromagnetic spectrum and (ii) demanding that the system's constituent chromophores exhibit significant overlap in their absorption and emission bands so that directional energy transfer can be realized. Biological systems overcome these problems in part through the utilization of a wide variety of pigments; Fig. 1 illuminates this point, displaying the electronic absorption spectra of the key chromophores involved in photon gathering in the chloroplasts of green plants.

In an effort to prepare new biomimetic light-harvesting systems that exhibit these properties, we have fabricated a variety of supramolecular, multichromophoric systems that have been hard-wired together by yne and polyynyl units. Ethyne, oligoethyne, and multiple ethyne bridges between porphyrins are the ideal linkage topologies to enable unusually high excitonic and electronic coupling between chromophore centers. Although the synthetic chemistry of the porphyrins is well developed, routes into appropriate yne-elaborated porphyrinic synthons suitable for development of such biomimetic supramolecular systems have been limited (*8*). We have recently demonstrated the general utility of metal-mediated cross-coupling as a powerful and versatile synthetic approach to both catalytically and quantitatively append a wide variety of organic moieties directly to the porphyrin periphery (*9*, *10*). This methodology is ideal for preparing a host of yne-elaborated porphyrin precursors as well as novel porphyrin arrays based on these units (*11*).

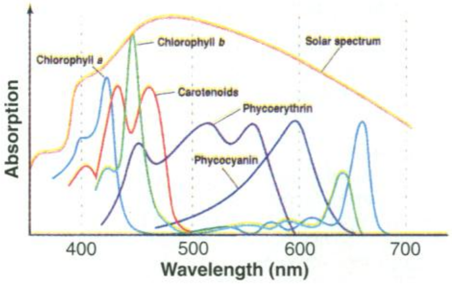

Fig. 1. The photosynthetic pigments and the solar spectrum. [Reprinted from (*34*) with permission © Wiley]

When appended directly to the porphyrin *meso* or β positions, the acetylenyl group allows significant modulation of ground- and excited-state optical and electronic properties; yne linkages between porphyrin units give rise to multichromophoric systems that display unusually strong excitonic coupling, exceptional electrochemical behavior, and phenomenally broad, high oscillator strength absorptions in the visible and near-infrared regions of the electromagnetic spectrum.

We report the electronic spectroscopy, electrochemistry, and room-temperature photophysics of three monomeric acetylenyl porphyrins as well as three prototypical porphyrinic arrays derived from these species that highlight the remarkable spectroscopic and electrochemical characteristics of these new classes of chromophoric structures. We have synthesized bis- and trisporphyrin arrays which are noteworthy in that the chromophores are linked by single ethyne bridges; the photophysical properties of these species have many features in common with the natural photosynthetic antenna systems. Additionally, we contrast herein the optical and electrochemical behavior of ethyne- and butadiyne-bridged porphyrins; the distinct spectroscopic and electronic properties afforded by each of these linkage motifs should be particularly useful in the developing chemistry and application of multichromophoric assemblies.

Electronic absorption spectroscopy. Metal-mediated cross-coupling techniques applied to appropriately halogenated porphyrin precursors allow the synthesis of an extended family of acetylenyl porphyrins (*12*); Fig. 2 shows three such molecules: (5-trimethylsilylethynyl-10,20-diphenylporphinato)zinc(II) (**1**), [5,15-bis(trimethysilylethynyl)-10,20-diphenylporphinato]zinc(II) (**2**), and (2-trimethysilylethynyl-5,10,15,20-tetraphenylporphinato)-zinc(II) (**3**). Appending an ethynyl moiety directly to the porphyrin carbon framework imparts distinctive features to the optical spectra of such molecules relative to the electronic spectra of more conventional *meso*-substituted metalloporphyrins. The

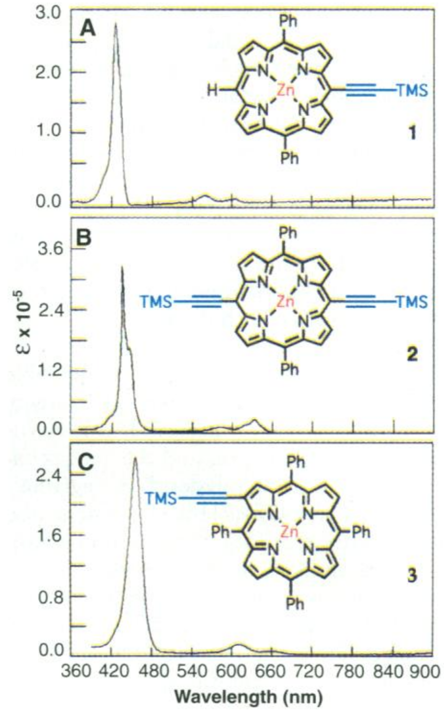

Fig. 2. Room-temperature electronic absorption spectra of molecules **1** (**A**), **2** (**B**), and **3** (**C**) in $CHCl_3$ solution.

full width at half maximum (FWHM) of the intense, high-energy Soret (B) transitions of (5,10,15,20-tetraphenylporphinato)zinc (ZnTPP) (Fig. 3A) and (5,15-diphenylporphinato)zinc (ZnDPP) (Fig. 3B) are narrow and correspond to energies of 747 and 719 cm^{-1}, respectively. In contrast, for both singly ethyne-elaborated porphyrins **1** and **3**, the B band transitions are broader (FWHM = 769 and 1032 cm^{-1}, respectively). The di-*meso* ethynyl porphyrin **2** has a clearly split B band. The splitting (506.9 cm^{-1}) between the B_x and B_y bands likely results from the removal of the degeneracy of the porphyrin *e* symmetry lowest unoccupied molecular orbital (LUMO), due directly to the cylindrically symmetric ethynyl groups fused to the porphyrin 5 and 15 positions. The pronounced disparity in oscillator strength stems from the increased conjugation along the C_2 molecular axis defined by the two ethynes. The *x*- and *y*-polarized transitions are not only energetically inequivalent; increased conjugation in one dimension results in one transition stealing oscillator strength from the other. Consistent with this model, the low-energy (wavelength $\lambda > 540$ nm) quasi-allowed (Q) transitions of both **1** and **2** show splittings not present in their parent compound, ZnDPP, with the disparity in oscillator strength between their respective low-energy absorptions dependent upon the number of ethyne moieties fused to the porphyrin *meso* position.

The authors are in the Department of Chemistry, University of Pennsylvania, Philadelphia, PA 19104–6323, USA.

*To whom correspondence should be addressed.

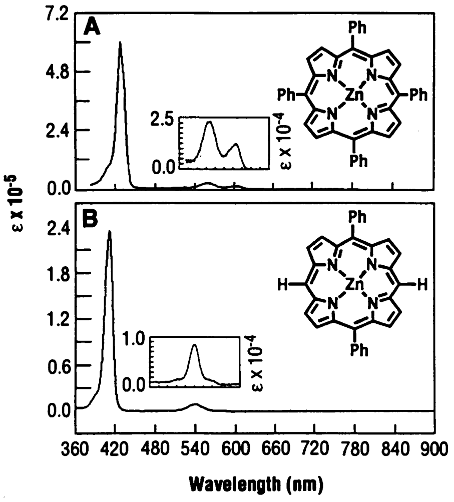

Fig. 3. Room-temperature electronic absorption spectra of (**A**) ZnTPP and (**B**) ZnDPP in $CHCl_3$ solution. Magnified views of the respective Q- band regions of these molecules are shown in the boxed insets.

Porphyrin molecules **1**, **2**, and **3** can be used as synthons in the fabrication of a variety of acetylenyl porphyrin arrays (*13*, *14*); representative structures include bis[(2,2′,-5,10,15,20-tetraphenylporphinato)-zinc(II)]butadiyne (**4**), bis[(5,5′,-10,20-diphenylporphinato)zinc(II)]ethyne (**5**), and 5,15-bis{[(5′-10,20-diphenylporphinato)-zinc(II)]ethynyl}[10,20-diphenylporphinato]zinc(II) (**6**). The structures and optical spectra of these yne-bridged porphyrin dimers and trimers are shown in Fig. 4. Molecule **4**, synthesized through an Eglinton reaction from (2-ethynyl-5,10,15,20-tetraphenylporphinato)zinc, shows several pronounced characteristics in the optical spectrum (Fig. 4A) that are distinct from a recently reported bisporphyrin system that features a butadiynyl bridge at the porphyrin *meso* position (*15*). Additionally, considerable structural information can be gleaned from the optical spectroscopy of **4** with respect to its previously synthesized nickel derivative (*16*). First, the high-energy region of the spectrum shows multiple optical transitions, with clearly discernible absorptions at 438.1, 460.1, and 489.8 nm. Second, relative to ZnTPP, the high-energy electronic transitions in **4** span a wide wavelength range (~380 → 510 nm) in which the FWHM is ~3000 cm^{-1}. Third, the energies of the absorption maxima in the Q-band region (611.9 and 569.5 nm) of **4** are essentially invariant with respect to the Q(0,0) and Q(1,0) absorptions of ZnTPP (603.4 and 563.7 nm, respectively). This latter point indicates that the porphyrins have essentially electronically decoupled ground states; given that a butadiyne wire links the two chromophores, we interpret this as evidence that the two porphyrins of **4** lie approximately orthogonal to each other. Splittings in the Soret region observed in the electronic spectra of dimeric porphyrins with small porphyrin-porphyrin spatial separations have generally been ascribed to excitonic coupling between the transition dipoles of the two chromophores (*17*). Such a B-bank excitonic splitting pattern, however, is inconsistent with a simple point-dipole description of a dimeric chromophore that features coplanar or noncoplanar interacting transition dipoles or both (*18*). Since neither a single geometric conformation nor a torsionally unrestricted bisporphyrin structure could account for the high energy region of **4**'s electronic spectrum, we believe that **4** exists at room temperature chiefly in a few conformationally preferred states in which the torsional angles between the chromophores are near 90°; such a hypothesis accounts for both the Q-band region as well as the notion that the observed large splittings in the blue region likely derive from excitonic interactions between the closely spaced chromophores. Vibronic coupling, however, may provide a possible alternative explanation for **4**'s optical spectrum. The transitions at 438.1 and 460.1 nm, as well as those at 460.1 and 489.8 nm, are separated by roughly 1200 cm^{-1}; a vibronic splitting of this magnitude is typically observed between the Q(0,0) and Q(1,0) transitions of simple fourfold symmetric porphyrins like ZnTPP. It is also curious to note that approximately 4125 cm^{-1} to the blue of the 569.5- and 611.9-nm transitions lie the 460.1- and 489.8-nm absorptions, signaling a possible vibronic genesis for the lower energy B-band features in the Q-band region of the spectrum. While both of these postulated vibronic origins for **4**'s B-band region are without previous experimental precedent, the large vibronic splitting required by the latter explanation make it highly improbable; the 4125 cm^{-1} separations between the absorptions are quite likely fortuitous (*19*, *20*).

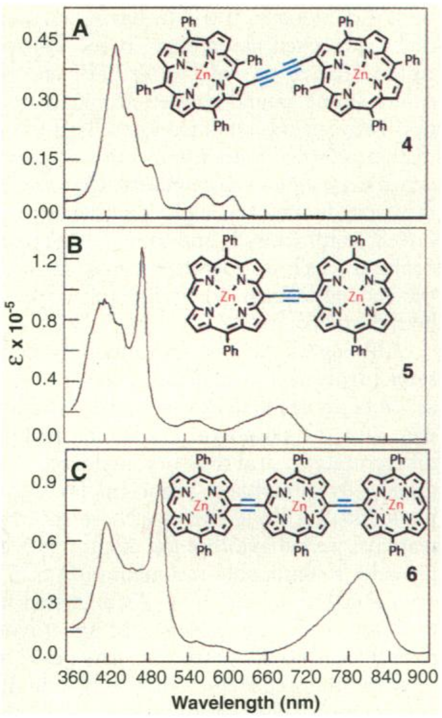

Fig. 4. Electronic absorption spectra of porphyrin arrays **4**, **5**, and **6** at room temperature in (**A**) $CHCl_3$, (**B**) $CHCl_3$, and (**C**) 10:1 $CHCl_3$:pyridine.

Palladium-catalyzed coupling of desilylated derivatives of **1** and **2** with (5-bromo-10,20-diphenylporphinato)zinc gave a porphyrin dimer with a single ethynyl bridge as well as a trimeric porphyrin that incorporates two yne linkages. In contrast to **4**, the optical spectrum of dimeric porphyrin **5** shows what appears to be a distinctly excitonically split Soret transition that features at least six well-defined absorptions; like that of **4**, the FWHM of **5**'s blue region of the electronic spectrum is broad (~4600 cm^{-1}). The low-energy region of the electronic spectrum has a number of distinctive characteristics. Again, multiple transitions are observable. The highest energy Q-type transition (552.5 nm) is slightly red-shifted relative to the reasonably intense Q(1,0) transition (~540 nm) of ZnDPP. A weaker absorption (625.1 nm), ~2100 cm^{-1} to the red of the 557.8-nm transition, is apparent and may signal that an yne stretching mode is vibronically coupled to the former excitation. Finally, at 683.4 nm lies the lowest energy transition in the ethyne-bridged porphyrin dimer, dramatically more intense [extinction coefficient (ε) = 23,250 M^{-1} cm^{-1}, FWHM ~2000 cm^{-1}] and substantially red-shifted relative to the analogous transition (λ = 540.4 nm, ε = 8780 M^{-1} cm^{-1}, FWHM = 905 cm^{-1}) in ZnDPP. The low-energy regime of the electronic spectrum of **5** sharply contrasts with that of **4**, in which the Q-type transitions are scarcely red-shifted relative to those of the parent monomer, ZnTPP. The electronic spectra of ZnDPP, **4**, and **5** indicate that the ethyne linkage motif between porphyrin chromophores should be particularly useful in the fabrication of supramolecular systems that feature low-energy, high oscillator strength transitions.

Such optical characteristics are further amplified in the electronic spectrum of the *meso* ethynyl-linked trimeric porphyrin structure **6**. Like **5**, **6** has an unusually split, very broad (FWHM = 4995 cm^{-1}) Soret region. The two sharpest transitions are split by 3812 cm^{-1} and are observed at 420.5 and 500.8 nm; this excitonic interaction is the largest such coupling yet reported for a synthetic multichromophoric compound and represents an increase over the largest such energetic splitting previously measured in solution of more than over 1000 cm^{-1} (*21*). Other less intense transitions are apparent at 437.0, 457.2, 464.5, and 490.9 nm. The 1906-cm^{-1} splitting between the 420.5- and 464.5-nm absorptions is the same as that between the 464.5- and 500.8-nm transitions, possibly indicating that a 1906-cm^{-1} mode is vibronically coupled to electronic excitation in this spectral region (*19*). A probable origin for such a vibrational spacing again lies with the ethynyl moieties that link the porphyrin units. When conjugated organic groups are bridged by an acetylene, the $C\equiv C$ stretching frequency, typically near 2150 cm^{-1}, can be considerably red-shifted. A 1906-cm^{-1} vibrational splitting would suggest that substantial electronic delocalization is provided by the porphyrins pendant to the ethynyl groups and that a cumulenic resonance form for the excited state of **6** may be significant (Scheme 1).

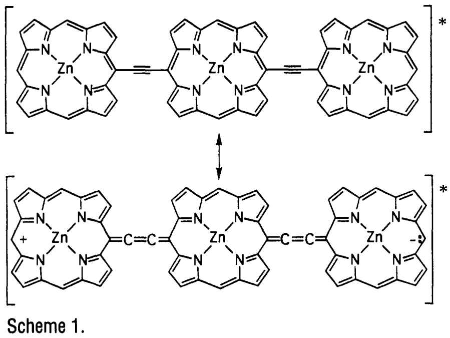
Scheme 1.

The low-energy spectral region of Fig. 4C shows a single absorption centered at 802.2 nm that tails well into the near-infrared; it is broad (FWHM = 1485 cm^{-1}) and intense ($\varepsilon = 42{,}800\ \mathrm{M}^{-1}\mathrm{cm}^{-1}$) and considerably red-shifted with respect to the low-energy optical transition observed for dimeric porphyrin **5**. Throughout the molecular series, ZnDPP-**1**-**2**-**5**-**6**, two trends become apparent: (i) the $\pi - \pi^*$ gap (taken as λ_{max} of the lowest energy transition) decreases regularly with increased conjugation and (ii) oscillator strength in the low-energy electronic transition increases concomitantly with the ability of the molecule to delocalize charge. The broadness of the lowest energy absorption in **6** underscores this latter point and suggests that this electronic excitation has more in common with a charge transfer transition than a proper Q band (*22*). This interpretation is of course consistent with the intriguing hypothesis that the excited state of **6** has a significant cumulenic resonance form.

Based on the optical spectra of **4**, **5**, and **6**, certain generalizations can be made regarding the relative structures of these molecules. The high-energy region of the absorption spectra of **5** and **6** is clearly distinct from that present in **4**. Additionally, **5** and **6**, having substantially red-shifted absorptions in the Q-band region relative to ZnDPP, ZnTPP, and **4**, evince strong ground-state electronic interaction between the chromophores. This information, coupled with the spectroscopic evidence suggesting some cumulenic character in the excited state of **6**, argues that the ethyne-linked porphyrins **5** and **6** are essentially coplanar. Such a structure is consistent with the general features of the B-band region of both **5** and **6**.

Although it may be appropriate to consider highly conjugated molecules **5** and **6** as "supermolecules" (that is, the ethynyl wire and the porphyrin cannot be strictly differentiated), and thus not amenable to a grossly oversimplified point-dipolar argument for describing the electronic spectral features, we believe that the exciton model provides a reasonable rationalization of **5**'s optical spectrum (*20, 23*). As discussed in the case of **3**, the presence of an ethyne moiety fused to the porphyrin *meso* position removes the degeneracy of the B_x and B_y transitions for the porphyrin chromophore. In **5**, for example, the two pairs of x- and y-polarized transitions of the individual chromophores would be expected to give rise to both parallel and in-line transition dipole interactions, producing four exciton states. Theory predicts both a highly allowed blue-shifted (B_y) and a highly allowed red-shifted (B_x) singlet-singlet electronic transition (with respect to the monomeric porphyrin) for electronic excitations to the exciton states generated from parallel and in-line transition dipole interactions, respectively, for a coplanar porphyrin geometry (*18*). These two key characteristics are manifest in the high-energy region of the optical spectrum of **5** as well as that of **6**. The slight broadening of the blue-shifted B_y transition with respect to B_x indicates the existence of molecular populations at room temperature that vary slightly from a perfectly coplanar chromophore arrangement, because the energy of a B_y transition is expected to have a dependence on the chromophore-chromophore torsional angle (*18*). The similarity of the extinction coefficients for the B_x and B_y transitions in both **5** and **6** also indicates that significant populations of yne-bridged dimers and trimers deviating substantially from near-zero torsional angles do not exist. Other factors that further complicate the B-band region of coplanar porphyrin arrays **5** and **6** likely include vibronic coupling, transitions to formally forbidden exciton levels, or both.

Because the magnitude of the $\pi - \pi^*$ gap in **4** varies little relative to that in ZnTPP, the chromophores in the butadiyne-linked dimer have little ground-state electronic interaction. Porphyrin arrays **5** and **6** thus stand in sharp contrast to array **4** in which the available spectroscopic evidence strongly suggests that **4**'s [porphinato]zinc units have an approximate orthogonal orientation (*24*).

Electrochemical data. Electrochemical data shown in Table 1 also support the structural assignments based on the optical data. Appending a single ethynyl group to the β position of ZnTPP or the *meso* position of ZnDPP has only a minor effect on the porphyrin ring oxidations, but significantly stabilize the one- and two-electron (1e and 2e) reduced forms of the porphyrin. For example, molecule **3**, bearing two *meso*-ethynyl moieties, is slightly more difficult to oxidize and substantially easier to reduce than its parent complex, ZnDPP. Ethynyl and butadiynyl linkage motifs give rise to substantially disparate porphyrinic electrochemical responses. For the ethyne-bridged porphyrin dimer **5**, each of the four porphyrin redox processes occurs in two 1e steps. For each redox process, substantial (120 to 260 mV) redox splitting occurs between

Table 1. Comparative electrochemistry of the acetylenyl porphyrins. $E_{1/2}$ is the half-wave potential. Cyclic voltammetric experimental conditions: [Porphyrin] = 2 mM; [$TBAPF_6$] = 0.15 M; solvent = benzonitrile; scan rate = 1.0 V/s; standard calomel reference electrode, platinum-disk working electrode; and an internal standard of ferrocene/ferrocenium (Fe^{II}/Fe^{III}) with a redox couple = 0.43 V.

Compound	$E_{1/2}$ (mV)			
	Ring oxidation		Ring reduction	
	ZnP/ZnP^+	ZnP^+/ZnP^{2+}	ZnP/ZnP^-	ZnP^-/ZnP^{2-}
ZnTPP	785	1168	−1388	−1773
ZnDPP	803	1200	−1413	−1800
1	738	1285	−1075	−1498
2	870	1260	−1100	−1570
3	870	1138	−1320	−1660
4	830*	1215*	−1300*	−1670*
5	620, 880	1300†	−1160, −1280	−1760, −1910

*Signifies a 2e redox step (all other redox processes are 1e in nature). †1e step—the associated second 1e step of second oxidation process occurs beyond the anodic solvent limit.

each of its constituent 1e steps. Significant redox splitting is a hallmark of strongly interacting ground-state redox centers and indicates that the resultant charge that accumulates on **5** throughout the course of the electrochemical experiment is considerably delocalized over both porphyrin centers. The ethynyl bridging motif thus causes the bisporphyrin system **5** to behave as a single redox entity.

This redox activity contrasts markedly to butadiynyl-bridged **4**, in which each redox process is 2e in nature. The 2e signature of **4**'s redox processes could indicate either redox cooperativity between the two porphyrin centers or complete electronic decoupling of the porphyrin units. The former case results when the second 1e step of the net 2e process is thermodynamically more facile that the initial 1e redox change; such could be the case if **4** is subject to redox-induced transformations of geometrical configuration. Because the anodic to cathodic peak-to-peak separations for each of the 2e redox processes in **4** are similar to the peak-to-peak separations (~100 mV) observed in the cyclic voltammetric responses of **5**, whose redox processes occur in discreet 1e steps, we feel that this interpretation of **4**'s redox behavior is less likely. A more plausible explanation for the 2e redox processes observed in the cyclic voltammetry of **4** is that geometric factors, such as porphyrin-porphyrin distance and porphyrin plane-porphyrin plane relative orientation, serve to electronically decouple the two redox units; the electrochemical responses observed are thus the superposition of two nearly noninteracting monomers. This behavior is in fact observed in bisporphyrin systems where the porphyrin planes have a face-to-face (cofacial) orientation when the porphyrin interplanar separations are large (*25*). These electrochemical responses are thus not inconsistent with our structural picture derived from the electronic spectra of these molecules, namely, that the chromophores in **4** are predominantly orthogonal whereas those in **5** are predominantly coplanar.

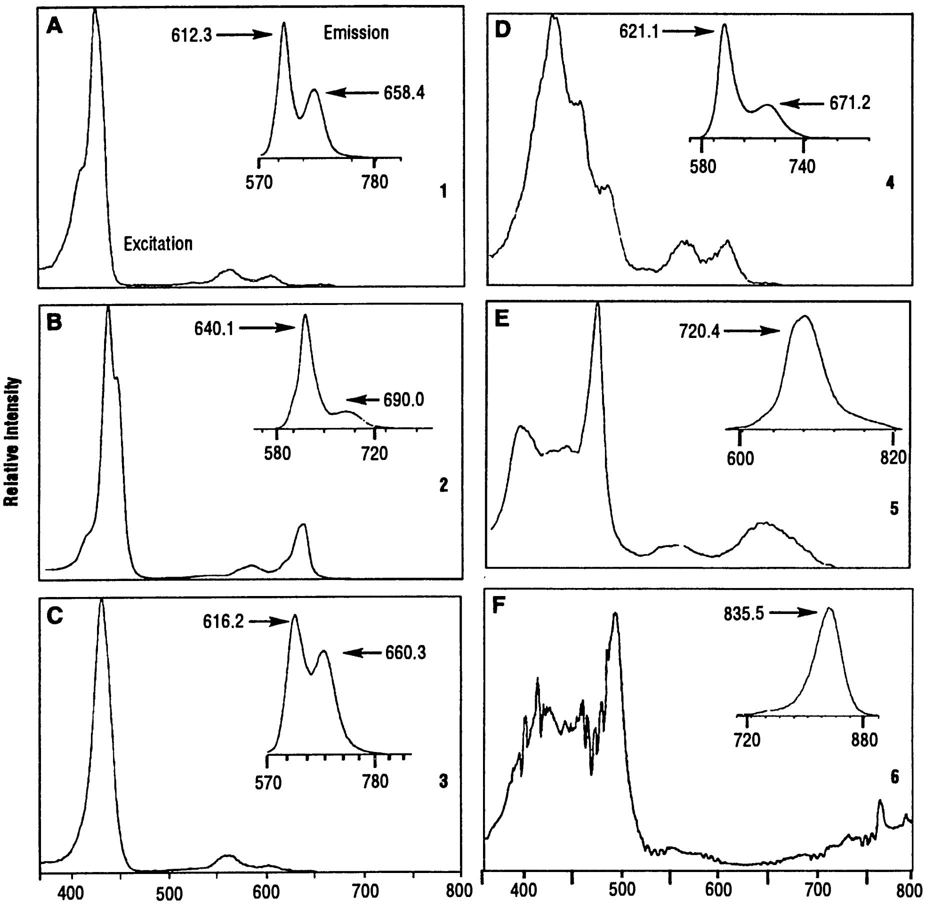

Fig. 5. Room-temperature excitation and emission spectra of molecules **1** to **6**. (**A**) Fluorescence excitation was monitored at 612 nm; λ_{ex} (emission) = 427 nm; $CHCl_3$ solvent. (**B**) Fluorescence excitation monitored at 640 nm; λ_{ex} (emission) = 431 nm; THF solvent. (**C**) Fluorescence excitation monitored at 616 nm; λ_{ex} (emission) = 431 nm; $CHCl_3$ solvent. (**D**) Fluorescence excitation monitored at 621 nm; λ_{ex} (emission) = 438 nm; $CHCl_3$ solvent. (**E**) Fluorescence excitation monitored at 720 nm; λ_{ex} (emission) = 478 nm; THF solvent. (**F**) Fluorescence excitation monitored at 835 nm; λ_{ex} (emission) = 500 nm; pyridine solvent.

Although the optical properties of these ethyne- and butadiyne-bridged porphyrins are unprecedented, these dimeric porphyrins are not the only bisporphyrin systems that exhibit strong electronic coupling between the ground-state chromophores; the cofacial porphyrin structural motif has been well studied and allows for such electronic interactions at small interporphyrin distances (*25, 26*). A comprehensive electrochemical survey of a large family of cofacial bis[(porphinato)zinc] complexes shows that the magnitude of redox splitting increases with decreasing porphyrin interplanar separation at a constant porphyrin-porphyrin relative orientation; the redox splitting for the ethyne-bridged porphyrin **5** exceeds that observed for even the most closely interacting cofacial bisporphyrin complexes (*25*). A more striking electrochemical property of the ethyne-bridged porphyrin arrays is the dramatic decrease in the HOMO-LUMO gap (taken as $E_{ox} - E_{red}$ of the first 1e oxidation and reduction) relative to the porphyrin monomer (that is, 1.78 V in **5** versus 2.21 V in ZnDPP). As Collman and co-workers pointed out in a qualitative molecular orbital analysis of bonding in cofacial porphyrin dimers, such porphyrin-porphyrin interactions result in only slight stabilization of the dimer LUMO relative to that of the monomer; the HOMO-LUMO gap for most cofacial bis[(porphinato)zinc] systems is thus seldom less than 2.0 V (*25*). Planar, yne-bridged porphyrin arrays thus represent a chromophore system with highly stabilized 1e reduced and oxidized forms.

Excitation and emission spectroscopy. For compounds **1** to **5**, the excitation spectra follow Kasha's rule and mirror the absorption spectra, as expected for pure compounds (Fig. 5, A to E). The excitation spectrum of the yne-bridged trimeric porphyrin, **6**, shows a curious feature (Fig. 5F): Although the emission intensity scales as expected at short wavelength (370 → 500 nm), there appears to be diminished signal intensity in the 800-nm region of the spectrum, possibly signaling that the excited state inefficiently converts to the emitting state.

As is observed in the emission spectrum of simple monomeric porphyrins, the emission spectra of compounds **1** to **4** (insets, Fig. 5, A to D) consist of two peaks that mirror the Q-band absorptions, shifted slightly to the red. The ethyne-bridged porphyrin dimer **5** exhibits a single unsymmetrical emission band a 720.4 nm, a longer wavelength than observed for the fluorescence emission of the less well electronically coupled, butadiyne-bridged dimeric porphyrin **4**. The highly conjugated trimeric porphyrin **6** emits even further to the red (λ_{em} = 835.5 nm) (inset, Fig. 5F). A notable aspect of the emission spectrum of **6** is its close energetic (497 cm^{-1}) proximity to the low-energy absorption centered at 802.2 nm; this Stokes shift is considerably smaller than that observed for **5** (752 cm^{-1}). The small Stokes shift signals highly "nested" ground- and excited-state potential surfaces, thus requiring minimal excited-state nuclear distortion with respect to the ground-state nuclear coordinates (*27*). Such is the case for monomeric porphyrins and the closely related chlorophylls, which typically show Stokes shifts on the order of a few hundred wave numbers (*28*). It might thus be expected that arrays of higher order than **6** should exhibit highly overlapping absorption and emission bands characteristic of the simple porphyrins and chlorophylls, but with the added feature of having readily tunable, low-energy absorptions that have high oscillator strengths.

Relevance to biological antenna molecules and light-harvesting assemblies. The design and fabrication of efficient photon-harvesting polymeric structures and materials necessarily precedes the development of artificial systems that could convert light energy into chemical energy (*29, 30*). The unusual optical spectra of these acetylenyl-bridged porphyrin compounds is further underscored when viewed alongside Fig. 1, and suggests their potential for use as precursors to such polymeric materials. The spectra shown in Fig. 4 indicate that an appropriately designed array consisting of ethyne- and butadiyne-bridged porphyrin structural elements may be able to mimic the chloroplast's essential light-harvesting multichromophoric spectral characteristics, accomplishing with a single chromophore (porphyrin) what the natural photon-gathering systems have required several pigments to effect.

Considerable effort has been spent in the elucidation of the biomimetic design criteria for antenna molecules; covalently linked porphyrin systems have figured prominently in such studies (*5, 30*). The suitability of these highly coupled porphyrins to such investigations is made obvious in the optical spectrum of trimeric porphyrin **6**, which is the first synthetic system that accurately models the salient spectroscopic characteristics of the B820 subunit of the core antenna complex (LH1) of the purple photosynthetic bacteria *Rhodospirillum rubrum, Rhodobacter capsulatus*, and *Rhodobacter sphaeroides* (*31*). Furthermore, compounds **5** and **6** bear many spectroscopic similarities to other purple bacterial light-harvesting complexes, as well as to the chlorosomes, the light-harvesting structures in green photosynthetic bacteria (*32*).

In addition to being new structural elements for developing the biomimetic chemistry of natural photosynthetic antenna systems, the unusual photophysical and electrochemical properties of these acetylenyl-bridged porphyrins lend themselves to a number of potential avenues for further investigation, including the development of near-infrared sensors, materials for nonlinear optics, novel higher order arrays and polymers, as well as new photosensitizing pharmaceuticals.

Note added in proof: Anderson (*33*) has recently reported a butadiyne bridged bisporphyrin system with a similarly large excitonic splitting.

REFERENCES AND NOTES

1. H. Nishide *et al., Macromolecules* **24**, 6306 (1991); H. L. Anderson and J. K. M. Sanders, *Agnew. Chem. Int. Ed. Engl.* **29**, 1400 (1991); N. Ushizawa and T. Shimomura, U.S. Patent 4,957,615 (1990); E. Tsuchida, H. Nishide, H. Kawakami, European Patent 0-464-717-A1 (1991).
2. B. A. Gregg, M. A. Fox, A. J. Bard, *J. Am. Chem. Soc.* **111**, 3024 (1989); M. Yoneyama, A. Fujii, S. Maeda, T. Murayama, *Chem. Lett.* **1991**, 929 (1991); E. M. McGhee, M. R. Godfrey, B. M. Hoffman, J. A. Ibers, *Inorg. Chem.* **30**, 803 (1991); M. P. O'Neil *et al., Science* **257**, 63 (1992); H. Segawa, N. Nakayama, T. Shimidzu, *J. Chem. Soc. Chem. Commun.* **1992**, 784 (1992); K. S. Suslick, C.-T. Chen, G. R. Meredith, L.-T. Cheng, *J. Am. Chem. Soc.* **114**, 6928 (1992); K. Sakoda, K. Kominami, M. Iwamoto, U.S. Patent 5,051,337 (1991); D. R. Terrell, S. K. De Meutter, B. Kaletta, European Patent 0-428-214-A1 (1991); L. R. Milgrom, World Intellectual Property Organization Patent WO 92/15099 (1992); S. C. Narang, S. Ventura, T. R. Bhardwaj, U.S. Patent 5,091,502 (1992).
3. J. S. Miller, J. C. Calabrese, R. S. McLean, A. J. Epstein, *Adv. Mater.* **4**, 498 (1992).
4. G. A. Schick, I. C. Schreiman, R. W. Wagner, J. S. Lindsey, D. F. Bocian, *J. Am. Chem. Soc.* **111**, 1344 (1989); T. Nagata, A. Osuka, K. Maruyama, *ibid.* **112**, 3054 (1990); A. Osuka *et al., Chem. Phys. Lett.* **181**, 413 (1991); A. Osuka *et al., J. Am. Chem. Soc.* **115**, 4577 (1993); J. Rodriguez *et al., ibid.* **113**, 1652 (1991); J. L. Sessler, V. L. Capuano, A. Harriman, *ibid.* **115**, 4618 (1993); D. Gust *et al., Science* **248**, 199 (1990); R. M. Hermant *et al., J. Am. Chem. Soc.* **115**, 2080 (1993); D. Gust *et al., ibid.*, p. 5684; M. R. Wasielewski *et al., ibid.* **112**, 6482 (1990); D. G. Johnson *et al., ibid.* **115**, 5692 (1993); E. Scamporrino and D. Vitalini, *Macromolecules* **25**, 1625 (1992); D. K. Luttrull *et al., Langmuir* **8**, 765 (1992); H. Segawa *et al., J. Phys. Chem.* **96**, 503 (1992).
5. S. Prathapan, T. E. Johnson, J. S. Lindsey, *J. Am. Chem. Soc.* **115**, 7519 (1993).
6. S. Anderson, H. L. Anderson, J. K. M. Sanders, *Acc. Chem. Res.* **26**, 469 (1993).
7. D. Kessel, Ed., *Photodynamic Therapy of Neoplastic Disease*, vols. I and II (CRC Press, Boca Raton, FL, 1990); R. K. Pandey, F.-Y. Shiau, C. J. Medforth, T. J. Dougherty, K. M. Smith, *Tetrahedron Lett.* **31**, 7399 (1990); M. Graça, H. Vicente, K. M. Smith, *J. Org. Chem.* **56**, 4407 (1991); R. K. Pandey, T. P. Forsyth, K. R. Gerzevske, J. J. Lin, K. M. Smith, *Teterahedron Lett.* **33**, 5315 (1992); K. R. Weishaupt, T. J. Dougherty, W. R. Potter, European Patent 0-161-606 (1985).
8. K. D. Smith, Ed., *Porphyrins and Metalloporphyrins*, (Elsevier, New York, 1975); J. B. Kim, A. D. Adler, F. R. Longo, *The Porphyrins*, D. Dolphin, Ed. (Academic Press, London, 1978), vol. 1, pp. 85–100; J. B. Paine, *ibid.*, pp. 101–234; J. S. Lindsey, I. C. Schreiman, H. C. Hsu, P. C. Kearney, A. M. Marguerettaz, *J. Org. Chem.* **52**, 827 (1987).
9. S. G. DiMagno, V. S.-Y. Lin, M. J. Therien, *J. Am. Chem. Soc.* **115**, 2513 (1993); *J. Org. Chem.* **58**, 5983 (1993).
10. V. S.-Y. Lin, S. G. DiMagno, M. J. Therien, manuscript in preparation; S. M. LeCours, S. G. DiMagno, M. J. Therien, manuscript in preparation.
11. Until recently, the only example of a porphyrin bearing an ethyne substituent was A. W. Johnson and co-workers' *meso*-ethynlyloctaethylporphyrin, isolated in ~80 percent purity from the dehydrohalogenation of *meso*-bromovinylporphyrin [D. P. Arnold, A. W. Johnson, M. Mahendran, *J. Chem. Soc. Perkin Trans.* 1, 366, (1978)]. Recently both Havesi and co-workers and Anderson have reported examples of acetylenyl porphyrins fabricated by various condensation methodologies [G. Proess, D. Pankhert, L. Hevesi, *Tetrahedron Lett.* **33**, 269 (1992); H. L. Anderson, *ibid.*, p. 1101]. Arnold and Nitschinsk have also explored metal-mediated cross-coupling as an alternative methodology into such systems and have reported a few examples of such structures [D. P. Arnold, L. J. Nitschinsk, *Tetrahedron Lett.* **34**, 693 (1993)]. Additionally, Lindsey and co-workers have used such an approach to append ethynyl moieties to the pendant phenyl rings of tetraaryl porphyrins to form diphenylethyne-linked supramolecular porphyrin systems [see (*5*)].
12. The molecules **1**, **2**, and **3** were synthesized in high yield (typically >90 percent isolated) through Pd-catalyzed cross-coupling of trimethylsilylethynylzinc chloride with (5-bromo-10,20-diphenylporphinato)zinc(II), (5,15-dibromo-10,20-diphenylporphinato)zinc(II), and (2-bromotetraphenylporphinato)zinc(II), respectively. Experimental methods were similar to those reported previously (*9*); the general synthetic approach is as follows: a 10-fold molar excess of the trimethylsilylethynylzinc chloride was transferred to a Schlenk-style storage tube containing ~0.10 mmol of (2-bromo-5,10,15,20-tetraphenylporphinato)zinc, (5-bromo-10,20-diphenylporphinato)zinc, or (5,15-dibromo-10,20-diphenylporphinato)zinc and 10 mg of $Pd(PPh_3)_4$ or Pd(dppf) [Ph, phenyl; dppf, 1,1′-bis(diphenylphosphinoferrocene)] catalyst in ~20 ml of tetrahydrofuran (THF). The total solvent volume was adjusted to 40 ml. The (bromoporphinato)zinc complex, Pd catalyst, and organometallic reagent were heated to 60°C in a sealed Schlenk tube under nitrogen. The time course of the reaction was monitored by thin-layer chromatography. At the endpoint [$t \sim 16$ and $t \sim 12$ hours, respectively, for $Pd(PPh_3)_4$ and Pd(dppf) catalyzed reactions], the mixture was then quenched with water, extracted with chloroform, dried over $CaCl_2$, and evaporated. Details for the isolation of each compound as well as selected characterization data are given below:
1: After completion of the $Pd(PPh_3)_4$-catalyzed cross-coupling reaction, the product was purified by column chromatography on silica gel with 1:9 THF:hexane. A brownish-red band was collected and evaporated. Isolated yield was 113 mg (91.5 percent based on 120 mg of the porphyrin starting material). Proton nuclear magnetic resonance (^1H NMR) (500 MHz, $CDCl_3$): δ 10.01 (s, 1 H), 9.99 (d, 2 H, coupling constant J = 4.0 Hz), 9.76 (d, 2 H, J = 4.4 Hz), 9.19 (d, 2 H, J = 3.7 Hz), 8.98 (d, 2 H, J = 4.3 Hz), 8.17 (m, 4 H), 7.76 (m, 6 H), and 0.61 (s, 9 H). ^{13}C NMR (125 MHz, $CDCl_3$): δ 152.09, 150.29, 149.78, 149.14, 142.27, 134.52, 132.72, 132.23, 131.70, 131.01, 127.54, 126.63, 121.23, 107.76, 107.17, and 0.43. Visible absorption bands (Vis) ($CHCl_3$): 427.5 (5.45), 519.9 (3.02), 560.5 (3.8), 604.2 (3.4) nm [log ε (extinction coefficient)]. Fast-atom bombardment mass spectrometry (FAB MS): 620 [calculated (calcd) 620]. Elemental analysis (Anal): Calcd for $C_{37}H_{28}N_4ZnSi$: C 71.43; H 4.54; and N 9.01. Found: C 71.22; H 4.49; and N 8.77.
2: After completion of the Pd(dppf) catalyzed cross-coupling reaction, the crude product was chromatographed on silica with 1:1 CH_2Cl_2:hexane as eluent. A dark green band was

isolated and evaporated to yield 45.1 mg of product (93 percent, based on 46 mg the porphyrin starting material). ^{1}H NMR (500 MHz, $CDCl_3$): δ 9.68 (d, 4 H, *J* = 4.6 Hz), 8.9 (d, 4 H, *J* = 4.7 Hz), 8.15 (m, 4 H), 7.76 (m, 6 H), and 0.58 (s, 18 H). ^{13}C NMR (125 MHz, $CDCl_3$): δ 0.32, 107.34, 115.08, 122.64, 126.67, 127.69, 131.29, 132.77, 134.39, 112.10, 150.26, and 152.22. Vis ($CHCl_3$): 437.0 (5.51), 446.9 (5.22), 539.3 (3.40), 582.2 (3.93), 621.8 (4.09), and 633.9 (4.35). FAB MS: 716 (calcd 716). Anal: Calcd for $C_{42}H_{34}N_4ZnSi_2$: C 70.43; H 4.78; and N 7.82. Found: C 70.11; H 4.69; and N 7.48.

3: Upon conclusion of the $Pd(PPh_3)_4$ catalyzed cross-coupling reaction, the product was purified by column chromatography on silica with 1:1 chloroform:hexane. A single red band was isolated and evaporated giving an isolated yield of 136.6 mg of the product (89.6 percent, based on 163 mg of the porphyrin starting material). ^{1}H NMR (500 MHz, $CDCl_3$): δ 9.20 (s, 1 H), 8.90 (d, 4 H, *J* = 4.13 Hz), 8.86 (d, 1 H, *J* = 4.4 Hz), 8.77 (d, 1 H, *J* = 4.4 Hz), 8.19 (m, 6 H), 8.11 (m, 2 H), 7.77 (m, 9 H), 7.66 (m, 3 H), and 0.22 (s, 9 H). Vis ($CHCl_3$): 430.9 (5.42), 559.0 (4.16), and 598.0 (3.67). FAB MS: 772 (calcd 772). A desilylated sample was analyzed. Anal: Calcd for $C_{46}H_{28}N_4Zn$: C 78.69; H 4.02; and N 7.98. Found: C 78.38; H 4.24; and N 7.69.

The compounds **1**, **2**, and **3** are readily desilylated to give the corresponding ethynyl-substituted porphyrins, which serve as synthons in further coupling reactions. In a typical desilylation reaction, 10 ml of a 1 M THF solution of tetrabutylammonium fluoride was added to 69 mg of **1** in 30 ml CH_2Cl_2 under nitrogen. The mixture was stirred for 50 min, quenched with water, extracted with chloroform, dried over $CaCl_2$, and evaporated. The product was purified by column chromatography on silica with 1:1 chloroform:hexane. Isolated yield = 54.9 mg of the desilylated product (90 percent yield, based on the silyl-protected ethynylporphyrin starting material). ^{1}H NMR (500 MHz, $CDCl_3$): δ 10.18 (s, 1 H), 9.75 (d, 2 H, *J* = 4.7 Hz), 9.28 (d, 2 H, *J* = 4.6 Hz), 8.96 (d, 2 H, *J* = 4.7 Hz), 8.94 (d, 2 H, *J* = 4.6 Hz), 8.21 (m, 4 H), 7.79 (m, 6 H), and 4.187 (s, 1 H). ^{13}C NMR (125 MHz, $CDCl_3$): δ 151.93, 150.14, 149.41, 149.11, 142.55, 134.23, 132.31, 131.75, 131.41, 130.29, 126.92, 126.06, 120.59, 107.29, 97.06, 86.79, and 77.21. Vis ($CHCl_3$): 424.0 (5.43), 558.0 (3.97), and 600.0 (3.5). FAB MS: 487 (calcd 487).

13. The compound **4** was synthesized through an Eglinton coupling of **3** with itself (*14*); **5** and **6** were synthesized through an additional Pd-catalyzed cross-coupling of an ethynyl-substituted porphyrin with an appropriate (bromoporphinato)zinc(II) species.

    4: An oven-dried 50-ml Schlenk tube equipped with a magnetic stirring bar was charged with (2-ethynyl-5,10,15,20-tetraphenylporphinato)zinc(II) (50 mg, 0.07 mmol) and 1.4 ml of prepurified pyridine. The solution was stirred under N_2 for 10 min. $Cu(OAc)_2$ (OAc, acetate; 40 mg, 0.2 mmol) in 2 ml of pyridine was heated to 60°C and added to the porphyrin-pyridine solution by syringe; the mixture was then warmed and stirred at 90°C for 1 hour. The solution was quenched with H_2O. A crude dark-green precipitate was collected, redissolved in $CHCl_3$, dried over $CaCl_2$, and purified by column chromatography on silica with 70:30 hexane:THF as eluent. A dark-green band was collected and evaporated to yield 38.3 mg of product (78 percent yield, based on the porphyrin starting material). Selected characterization data: ^{1}H NMR (500 MHz, $CDCl_3$, 320 K): δ 9.15 (br. s, 2 H), 8.74 (m, 12 H), 8.11 (m, 16 H), and 7.65 (m, 24 H). Vis ($CHCl_3$): 438.1 (4.64), 460.1 (4.44), 489.8 (4.16), 569.5 (3.8), and 611.9 (3.76). FAB MS: 1398 (calcd 1398).

    5: Lithium bistrimethylsilylamide (1 mmol) was added to a solution of (5-ethynyl-10,20-diphenylporphinato)zinc(II) (50 mg, 0.1 mmol) in 20 ml THF to yield the (5-ethynyllithium-10,20-diphenylporphinato)zinc(II) reagent. (5-bromo-10,20-diphenylporphinato)zinc(II) (60 mg, 0.1 mmol) and 10 mg of $Pd(PPh_3)_4$ in 20 ml THF were added to this solution by canula. After completion of the metal-mediated cross-coupling reaction, chromatography was carried out on silica with 9:1 hexane:THF as eluent. The first green band was isolated and evaporated to yield 77.2 mg of the product (yield = 72 percent, based on (5-ethynyl-10,20-diphenylporphinato)zinc(II)). ^{1}H NMR (250 MHz, $CDCl_3$): δ 10.43 (d, 4 H, *J* = 4.6 Hz), 10.03 (s, 2 H), 9.21 (d, 4 H, *J* = 4.4 Hz), 9.06 (d, 4 H, *J* = 4.5 Hz), 8.91 (d, 4 H, *J* = 4.4 Hz), 8.22 (m, 8 H), and 7.72 (m, 12 H). Vis ($CHCl_3$) 413.9 (4.96), 420.5 (4.97), 426.0 (4.96), 432.6 (4.92), 445.8 (4.89), 477.7 (5.1), 549.2 (4.15), 552.5 (4.14), 557.8 (4.15), 625.1 (4.09), and 683.4 (4.37). FAB MS: 1070 (calcd 1070).

    6: $Pd(PPh_3)_4$ (20 mg, 0.0173 mmol) and CuI (10 mg) were added to a solution of (5-bromo-10,20-diphenylporphinato)zinc(II) (120 mg, 0.2 mmol) in 20 ml THF. (5,15-diethynyl-10,20-diphenylporphinato)zinc(II) (57 mg, 0.1 mmol) and 0.35 ml of diethylamine in 20 ml THF were added to this solution by canula. After completion of the metal-mediated cross-coupling reaction, the precipitated product was isolated by filtration and then recrystalized from a pyridine-hexane mixture to give 66.5 mg of the product (yield = 41 percent based on the (5,15-diethynyl-10,20-diphenylporphinato)zinc(II) starting material). ^{1}H NMR (500 MHz, $CDCl_3$): δ 10.86 (d, 4 H, *J* = 4.5 Hz), 10.78 (d, 4 H, *J* = 4.4 Hz), 10.39 (s, 2 H), 9.50 (d, 4 H, *J* = 4.3 Hz), 9.42 (d, 4 H, *J* = 4.4 Hz), 9.32 (d, 4 H, *J* = 4.8 Hz), 9.15 (d, 4 H, *J* = 4.0 Hz), 8.52 (m, 4 H), 8.47 (m, 8 H), 7.89 (m, 6 H), and 7.85 (m, 12 H). Vis (10:1 $CHCl_3$:pyridine): 420.5 (4.84), 437.0 (4.72), 457.2 (4.66), 464.5 (4.66), 490.9 (4.85), 500.8 (4.95), 552.0 (3.99), and 802.2 (4.63). FAB MS: 1616 (calcd 1616).
14. G. Eglinton and W. McCrae, *Adv. Org. Chem.* **4**, 225 (1963).
15. D. P. Arnold and G. A. Heath, *J. Am. Chem. Soc.* **115**, 12197 (1993).
16. D. P. Arnold and L. J. Nitschinsk, *Tetrahedron* **48**, 8781 (1992).
17. R. Selensky, D. Holten, M. W. Windsor, J. B. Paine III, D. Dolphin, *Chem. Phys.* **60**, 33 (1981); A. Osuka and K. Maruyama, *J. Am. Chem. Soc.* **110**, 4454 (1988); C. A. Hunter, J. K. M. Sanders, A. J. Stone, *Chem. Phys.* **133**, 395 (1989); S. Eriksson, B. Kållebring, S. Larsson, J. Mårtensson, O. Wennerstrom, *ibid.* **146**, 165 (1990); O. Bilsel *et al.*, *J. Am. Chem. Soc.* **114**, 6528 (1992); P. Jaegermann, M. Plato, B. vanMaltzan, K. Mobius, *Mol. Phys.* **78**, 1057 (1993).
18. M. Kasha, H. R. Rawls, M. A. El-Bayoumi, *Pure Appl. Chem.* **11**, 371 (1965).
19. Resonance Raman excitation profiles coupled with low-temperature spectroscopic studies would provide important information necessary to unambiguously assign the optical transitions.
20. Molecular orbital and electronic structure calculations would be required in order to provide a more quantitative description of the photophysical properties of porphyrin arrays **4**, **5**, and **6**.
21. N. Berova, D. Gargiulo, F. Derguini, K. Nakanishi, N. Harada, *J. Am. Chem. Soc.* **115**, 4769 (1993).
22. The solvatochromic behavior of the 802.2-nm absorption of **6** is consistent with its assignment as a charge-transfer band; V. S.-Y. Lin and M. J. Therien, unpublished results.
23. Although the exciton model provides a framework in which to rationalize the spectra, it significantly underestimates the magnitude of the B-band splitting because of the large interporphyrin electronic overlap enabled by the bridging acetylene unit.
24. Molecular modeling studies indicate that such a structure is reasonable.
25. Y. Le Mest, M. L'Her, N. H. Hendricks, K. Kim, J. P. Collman, *Inorg. Chem.* **31**, 835 (1992).
26. N. E. Kagan, D. Mauzerall, R. B. Merrifield, *J. Am. Chem. Soc.* **99**, 5484 (1977); J. P. Collman *et al.*, *ibid.* **105**, 2694 (1983); C. K. Chang and I. Abdalmuhdi, *Angew. Chem. Int. Ed. Engl.* **23**, 164 (1984).
27. N. J. Turro, *Modern Molecular Photochemistry*, (Benjamin/Cummings, Menlo Park, CA, 1978).
28. J. Hevesi and G. S. Singhal, *Spectrochim. Acta* **25A**, 1751 (1969); M. Gouterman, in *The Porphyrins*, D. Dolphin, Ed. (Academic Press, London, 1978), vol. 3, pp. 1–165.
29. S. E. Webber, *Chem. Rev.* **90**, 1469 (1990).
30. M. A. Fox, W. E. Jones, D. M. Watkins, *Chem. Eng. News* **71** (no. 11), 38 (1993).
31. R. W. Visschers *et al.*, *Biochem. Biophys. Acta.* **1100**, 259 (1992).
32. D. E. Tronrud, M. F. Schmid, B. W. Matthews, *J. Mol. Biol.* **188**, 443 (1986); G. J. S. Fowler, W. Crielaard, R. W. Visschers, R. vanGrondelle, C. N. Hunter, *Photochem. Photobiol.* **57**, 2 (1993); K. Matsuura, M. Hirota, K. Shimada, M. Mimuro, *ibid.*, p. 92.
33. H. L. Anderson, *Inorg. Chem.* **33**, 972 (1994).
34. D. Voet and J. G. Voet, *Biochemistry* (Wiley, New York, 1990), p. 591.
35. We dedicate this article in memory of T. G. Traylor. M.J.T. is indebted to the Searle Scholars, Beckman Young Investigator, and National Science Foundation Young Investigator (CHE93-57130) Programs as well as the National Institutes of Health (GM 48130-01A1.4) for generous financial support. We thank H. Holden Thorp for his assistance in obtaining excitation spectrum 5F.

14 February 1994; accepted 15 April 1994